Determination of Micro- and Nano-particle Properties by Multi-Frequency Bayesian Methods and Applications to Nanoelectrode Array Sensors

A. Cossettini[1], B. Stadlbauer[2], J. A. Morales E.[2], L. Taghizadeh[2], L. Selmi[3], and C. Heitzinger[2]
[1]DPIA, University of Udine, Udine, Italy, email: cossettini.andrea@spes.uniud.it
[2]Department of Mathematics and Geoinformation, TU Wien, Vienna, Austria
[3]DIEF, University of Modena and Reggio Emilia, Modena, Italy

***Abstract*—We demonstrate a new and robust Bayesian estimation method to extract properties of micro- and nano-scale analytes from measurements on advanced high-frequency impedance spectroscopy nanoelectrode array sensors. Firstly, the method is validated on model systems of a-priori known properties using accurate analytical and numerical models in place of actual measurements. Then, applications to real measurements with an advanced CMOS sensor demonstrate the usefulness of the methodology for robust and fast estimation of multi-dimensional parameters and parameter uncertainty in the context of biosensing and possibly sensor-fusion problems.**

***Keywords*— Nanoelectrode sensors, Bayesian estimation**

I. Introduction

High-frequency impedance spectroscopy (bio-)sensors with high surface density of micro/nanoelectrodes (i.e., high spatial resolution) can image analytes located beyond the thin Debye screening layer boundary in physiological electrolytes [1, 2, 3, 4, 5]. While the in-plane analyte geometry can be extracted with conventional image processing algorithms [6], simultaneous extraction of the out-of-plane elevation and of the electrical properties of the analyte and the environment remains challenging at the micro- and nano-scale. In fact, a reliable electrical model of the physical transduction mechanism is necessary, while noise and fluctuations limit the precision.

The extraction of analyte properties can be addressed by classical inverse-modeling techniques [7, 8]. However, since these techniques rely on minimizing the gap between models and experiments, they always yield deterministic parameter values, whose correctness and sensitivity must be assessed separately, as ill-posed nonlinear inversions may not have unique solutions.

In this work, we propose to treat the unknown parameters in a partial differential equation (PDE) model of the biosensor as random variables. The known physics is described by the PDEs, while the unknown parameters are described correctly in the framework of probability theory. Starting with modified Markov Chain Monte Carlo techniques (MCMC, [9]), we then develop a new powerful and robust Bayesian estimation method, well suited to support quantitative measurements useful for direct identification and metrology of micro- and nano-scale analytes.

The advantage of this approach is that we obtain probability distributions for the parameters, which inform us how reliable the results are, and the respective confidence intervals, which are precious information to achieve in the field of biosensors. Application to parameter estimation for micro- and nano-particle properties measured by nanoelectrode array sensor devices demonstrates the ability of the method to identify particle size, location, and the electrolyte dielectric properties.

This research was supported in part by the FLAG-ERA CONVERGENCE project via the Italian MIUR and the IUNET Consortium, and by the FWF (Austrian Science Fund) START Project no. Y660 PDE Models for Nanotechnology.

II. The Physical System

Our case study is the nanoelectrode array sensor of [1, 2, 5] sketched in **Fig. 1**. It features a dense matrix of 256x256 AuCu nanoelectrodes (180nm diameter) fabricated by dedicated post-processing of a 90 nm LP-CMOS technology by TSMC. On-chip temperature sensors, readout circuitry, A/D conversion and serial interface, temperature control and microfluidics to/from the ≈50 nL fluidic chamber complete the system. The platform measures the electrode capacitance in the 1.6–70 MHz band. *Ad-hoc* calibrations correct for systematic errors [5]. The output signal is the capacitance change, ΔC, induced by the presence of particles (analytes) and is available with ≈9 bits resolution [5].

III. Numerical and Analytical Models

Calculations employ the ENBIOS code [10, 11, 12], which solves the Poisson-Drift-Diffusion system of PDEs in 3D in the AC small-signal regime and allows us to precisely compute ΔC even for small analytes [13]. An accurate analytical model consistent with the above PDEs [14] predicts a nanoelectrode response to a particle proportional to the squared unperturbed electric field $\tilde{\boldsymbol{E}}_{\boldsymbol{0}}$ at the particle location. This model, extensively validated in [14], has been used to accelerate the calculations described in Sect. 4. The analytical model agrees well with ENBIOS in the limit of a small particle volume, as shown in **Fig. 2** for varying particle radius r_p and elevation d_z.

IV. Bayesian Estimation

Bayes' Theorem in probability density function (pdf) form for inverse problems states that given a prior initial guess of the parameter(s) distribution $\pi_0(q)$, consecutive random measurements y can be used to refine the posterior parameter pdf according to the expression $\pi(\mathrm{q}|\mathrm{y}) = \pi(\mathrm{y}|\mathrm{q})\pi_0(\mathrm{q})/\pi(y)$.

We develop our method starting with a Metropolis-Hastings (MH) implementation of the MCMC that avoids the calculation of computationally heavy probability integrals, while exploring the right regions of the distribution. The MH algorithm is [9]:

for k=1:$N_{samples}$

- Propose a parameter value q^* according to $J(q_{k-1}, q^*)$;
- Compute acceptance ratio α:

$\alpha=\min\{1,L(y|q^*)\pi_0(q^*)J(q^*,q_{k-1})/[L(y|q_{k-1})\pi_0(q_{k-1})J(q_{k-1},q^*)]\}$;

978-1-7281-1634-1/19/$31.00 ©2019 IEEE

• Cast a uniformly distributed χ in [0,1];
• Accept proposal if $\chi<\alpha$, else $q_k := q_{k-1}$.

Result: mean $\langle q \rangle = \Sigma q_k / N_{samples}$ & posterior distribution $\pi(q|y)$.

Here we have used a uniform distribution as prior (i.e., best uninformed choice), and a normal distribution as the likelihood $L(y|q)$ and the proposal functions $J(q, q')$. The likelihood function for a given measurement y is computed using either the analytical or numerical model so that, for a normal distribution, we have $L(y|q)=\exp(-(y-y_M(q))^2/2\sigma_L)$, where σ_L is the variance and $y_M(q)$ is the output generated by the model using the parameter(s) q. Unless otherwise stated, we will use $N_{samples}=10^5$ and likelihood factors $\sigma_L = 5 \cdot 10^{-5}$ consistent with the expected resolution. In order to obtain better convergence to the true posterior, in this work the Delayed Rejection Adaptive Metropolis (DRAM) algorithm (which is no longer a Markov Chain) has been used [15, 16]. Delayed Rejection (DR) gives alternative candidates q^*_j if the first one q^* is rejected instead of immediately keeping the previous q_{k-1}. The Adaptive Metropolis (AM) modification provides an updated covariance matrix for a normal distribution used as the proposal function for the second candidates q^*_2, etc. Thus, DR alters the proposal temporarily to stimulate mixing, whereas AM updates the proposal by learning information about the posterior. The flowchart of our method is shown in **Fig. 3**. Thanks to this improved Bayesian inference algorithm, a much smaller number of samples is required to reach convergence (**Fig. 4**), thus saving measurement time, since less measured data have to be acquired.

V. Implementation and Verification

In this section, we prove the effectiveness of our method on simulated data, for which the extracted values of the parameters q can be compared directly to the values known *a-priori*. We start considering a particle suspended above the center of *one* electrode (r_{el}=90 nm, d_x=d_y=0) and we use the analytical model to compute the likelihood function. **Fig. 5** shows color maps and marginal distributions of the posterior distribution for the simultaneous estimation of the particle radius r_p and vertical position d_z+r_p, with $\sigma_L = 5 \cdot 10^{-5}$, consistent with ≈9 bits resolution (yellow corresponds to high probability). The extracted mean values (r_p =48 nm, d_z+r_p=171 nm) are in good agreement with the exact ones (r_p =50 nm, d_z+r_p=150 nm). The residual difference is partly due to the slight error of the analytical model compared to the reference ENBIOS solution used to calculate $\tilde{\boldsymbol{E}}_0$, consistently with **Fig. 2,** and the limited resolution.

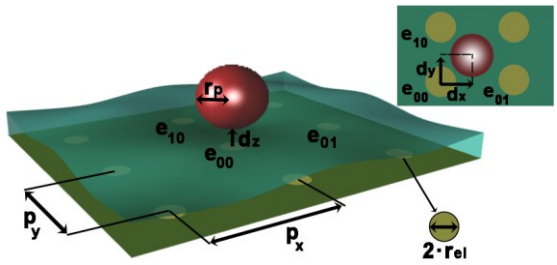

Fig. 1. Sketch of the nanoelectrode array sensor with a free-standing particle on top, and definitions of the main geometrical parameters: electrode radius (r_{el}=90 nm), particle radius (r_p), particle elevation (d_z) and lateral displacements (d_x, d_y), electrode pitch (p_x=600 nm, p_y=890 nm). We label e_{00} the electrode closest to the particle (highest ΔC), e_{01} and e_{10} the first neighbors in the row (x) and column (y) directions, respectively.

In fact, if $\tilde{\boldsymbol{E}}_0$ becomes more uniform, as assumed by the analytical model (e.g. by considering a larger electrode, r_{el} =200 nm, a smaller r_p =10 nm, and d_z=10 nm and an almost ideal measurements accuracy, σ_L =10^{-17}), then the estimate coincides with the true value without uncertainty (not shown). These results demonstrate the ability of the method to reliably estimate the size and vertical position of the nanoparticle.

To validate further the methodology, we investigate multi-parameters estimations of geometrical and electrical properties using the response at the electrodes e_{00}, e_{01} and e_{10} identified in **Fig. 1**. **Fig. 6** shows the results of a 5-parameters estimation (d_x, d_y, d_z, r_p, ε_p). Here as well very good agreement is obtained between estimated (0.28 nm, 0.01 nm, 151 nm, 50.5 nm, 2.5) and nominal (0 nm, 0 nm, 150 nm, 50 nm, 2.6) values, confirming the ability of the methodology to support nanoparticle metrology.

VI. Parameter Estimation from Experiments

Fig. 7 reports color maps of the experimental ΔC measured by the sensor array of [5] following insertion in the microfluidic chamber of SiO_2 based particles dispersed in NaCl 10mM electrolyte (Sigma-Aldrich, r_p=2.5±0.1 µm). Each pixel represents one nanoelectrode. We observe spots where either individual particles (A) or agglomerates (B) are present, either suspended or attached to the surface. To gain better insight on their actual nature, we use the multi-frequency estimation procedure (f=1.6-70 MHz) to the ΔC measurement and full 3D ENBIOS simulations as the model for L(y|q). **Fig. 8** shows size, position and electrolyte salt concentration estimations for objects "A" and "B". While the ones for "A" are consistent with the expectations from one particle, those for "B" confirm and quantify the anomalous nature of the underlying analyte. Finally, **Fig. 9** compares experimental ΔC spectra for particle "A" to those simulated using the extracted parameters, thus corroborating the validity of the extracted values.

VII. Conclusions

The extensive analysis demonstrates that the proposed estimation method can reveal important properties of nanoparticles and their environment from impedance measurements at nanoelectrode arrays. The technique thus appears very promising to address complex metrology problems at the nanoscale by purely electrical measurements.

Acknowledgments

The authors thank F. Widdershoven (NXP Semiconductors) and S. G. Lemay (Univ. of Twente) for insightful discussions, M. C. Nicoli and M. Anese (Univ. of Udine) for support with the measurements.

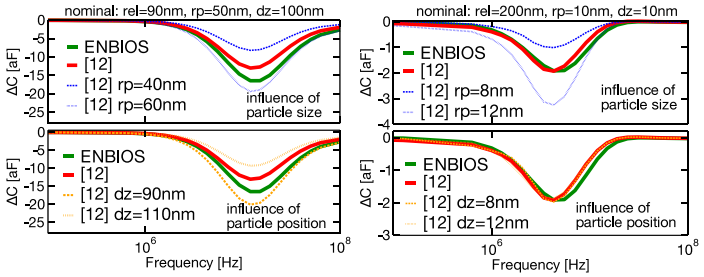

Fig. 2. ΔC spectra computed with ENBIOS and with the analytical model of [14] with $\tilde{E}_0$ (unperturbed field at the particle location) taken from ENBIOS. 100 mM NaCl electrolyte. Left: r_{el}=90 nm, r_p=50 nm, d_z=100 nm; the model inaccuracy w.r.t. ENBIOS entails Δ≈10 nm uncertainty. Right: r_{el}=200 nm, r_p=10 nm, d_z=10 nm; Δ ≈1 nm (a smaller r_p and larger r_{el} entail a more uniform $\tilde{E}_0$ as assumed by the model).

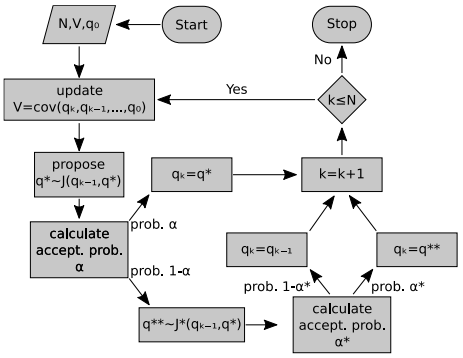

Fig. 3. Flowchart of DRAM method implemented in this work. q is the parameter (vector) to estimate.

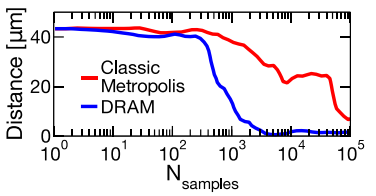

Fig. 4. Comparison between DRAM (this work) and MCMC ([9]) methods to estimate 2 parameters (r_p=11 μm, d_z=10 nm). The Euclidean distance between the extracted and the exact value is used to identify convergence. DRAM requires a much smaller number of samples to converge.

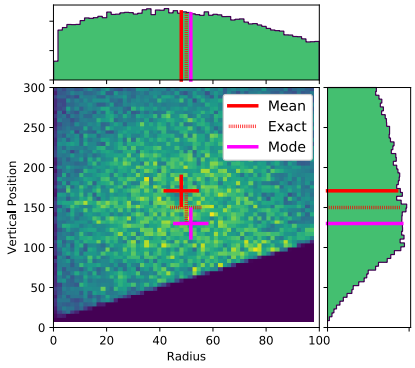

Fig. 5. 2D color map of posterior distribution for the simultaneous estimation of radius (r_p) and vertical position (d_z+r_p) of a particle floating in NaCl 10 0mM electrolyte above the center of an electrode using 32 frequency points in the f=1 kHz-1GHz range. Yellow means high probability. Parameters: r_p=50 nm, d_z=100 nm, σ_L=5·10^{-5}.

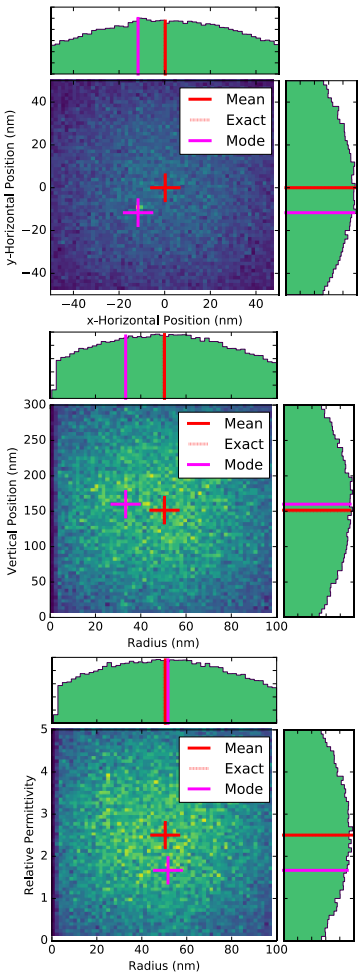

Fig. 6. Color maps of the posterior distributions for 5 parameters estimation (d_x, d_y, d_z, r_p, ε_p) of a r_p=50 nm spherical dielectric particle with relative permittivity ε_p=2.6, located in (0,0,150 nm). Top: marginal 2D histogram for (d_x, d_y). Center: same for (r_p, r_p+ d_z). Bottom: same for (r_p, ε_p). The estimation uses the multi-frequency information at the three electrodes e_{00}, e_{01}, e_{10}, which improves a lot the accuracy compared to Fig. 5 (mean very close to exact value) for the same σ_L=10^{-5}. Bayesian estimation suppresses noise by maximizing the pdf and narrowing its width. This process improves the precision and can be accelerated by means of iterative techniques.

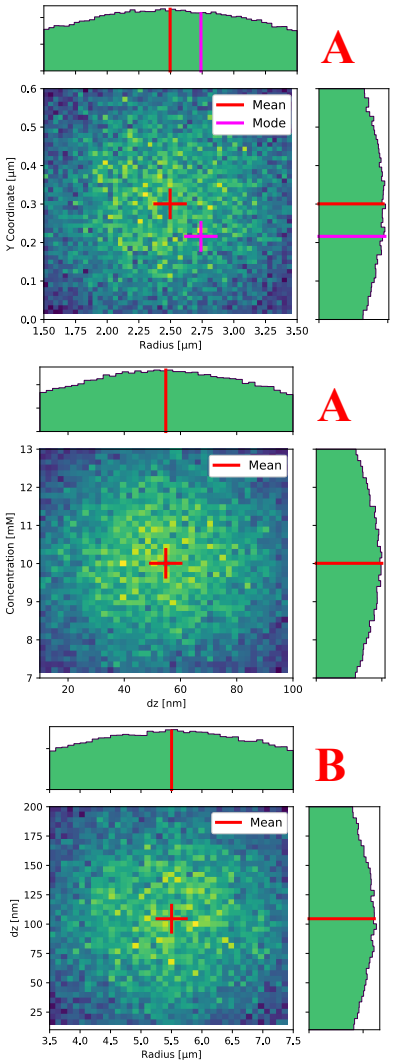

Fig. 8. Method of this work applied to object "A" (top and center) and "B" (bottom) in Fig. 7. Top: estimation of r_p and d_y. The extracted radius (2.5μm) is consistent with the expected size of one particle. Center: estimation of vertical elevation and salt concentration of the (nominally, 10mM) electrolyte solution. Bottom: estimation of r_p and d_z; the extracted radius (5.5μm) and elevation confirm that the nature of the measured signal is likely that of an agglomerate. σ_L=10^{-5} consistently with the 9 bits resolution of the nanoelectrode array sensor [5].

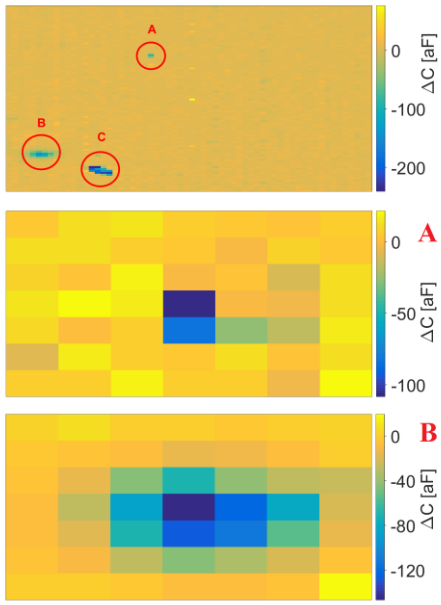

Fig. 7. Top: experimental 2D map of the array in NaCl 10mM with microparticles at 70 MHz. Red circles identify possible particles or particle-agglomerates. Center: zoom over "A", likely a single particle. Bottom: zoom over "B", likely an agglomerate of particles.

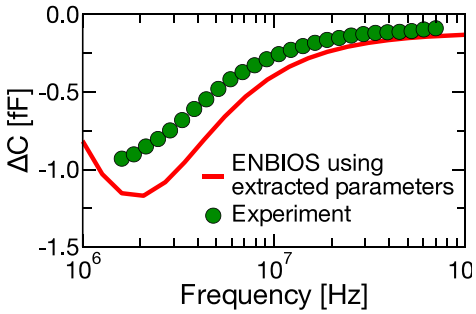

Fig. 9. Capacitance spectra at electrode e_{00} of the experiments compared to the capacitance spectra simulated by ENBIOS, using the parameters extracted in Fig. 8, for object "A".

REFERENCES

[1] C. Laborde *et al.*, "Real-time imaging of microparticles and living cells with CMOS nanocapacitor arrays," *Nature Nanotechnology*, vol. 10, no. 9, pp. 791–795, 2015, doi: 10.1038/nnano.2015.163.

[2] S. G. Lemay *et al.*, "High-frequency nanocapacitor arrays: Concept, recent developments, and outlook," *Accounts of Chemical Research*, vol. 49, no. 10, pp. 2355–2362, 2016, doi: 10.1021/acs.accounts.6b00349.

[3] V. Viswam *et al.*, "High-density CMOS microelectrode array system for impedance spectroscopy and imaging of biological cells," in *Proc. IEEE SENSORS*, 2016, pp. 1–3, doi: 10.1109/ICSENS.2016.7808761.

[4] C. M. Lopez *et al.*, "A 16384-electrode 1024-channel multimodal CMOS MEA for high-throughput intracellular action potential measurements and impedance spectroscopy in drug-screening applications," in *Proc. 2018 IEEE International Solid-State Circuits Conference - (ISSCC)*, Feb 2018, pp. 464–466, doi: 10.1109/ISSCC.2018.8310385.

[5] F. Widdershoven *et al.*, "A CMOS pixelated nanocapacitor biosensor platform for high-frequency impedance spectroscopy and imaging," *IEEE Transactions on Biomedical Circuits and Systems*, vol. 12, pp. 1369–1382, Dec 2018, doi: 10.1109/TBCAS.2018.2861558.

[6] W. K. Pratt, "Digital Image Processing", *Wiley*, 1991.

[7] M. Kern, "Numerical Methods for Inverse Problems", *Wiley*, 2016.

[8] H. W. Engl and P. Kügler, "Nonlinear inverse problems: theoretical aspects and some industrial applications," in *Multidisciplinary methods for analysis optimization and control of complex systems*, pp. 3–47, Springer, 2005, doi: 10.1007/3-540-27167-8_1.

[9] B. Stadlbauer *et al.*, "Bayesian estimation of physical and geometrical parameters for nanocapacitor array biosensors," *Journal of Computational Physics*, vol. 397, pp. 108874, Nov 2019, doi: 10.1016/j.jcp.2019.108874.

[10] F. Pittino and L. Selmi, "Use and comparative assessment of the CVFEM method for Poisson-Boltzmann and Poisson-Nernst-Planck three dimensional simulations of impedimetric nano-biosensors operated in the DC and AC small signal regimes," *Computational Methods in Applied Mechanics and Engineering*, pp. 902–923, 2014, doi: 10.1016/j.cma.2014.06.006.

[11] P. Scarbolo, F. Pittino, M. Dalla Longa, A. Cossettini, and L. Selmi, "ENBIOS-1D Lab," Apr 2017. v3.0. [Online]. Available: https://nanohub.org/resources/biolab, doi: 10.4231/D3Z02Z963.

[12] A. Hoxha, P. Scarbolo, A. Cossettini, F. Pittino, and L. Selmi, "ENBIOS-2D Lab," Oct 2016. v1.0. [Online]. Available: https://nanohub.org/resources/biolabisfet, doi: 10.4231/D3V11VM7D.

[13] A. Cossettini and L. Selmi, "On the response of nanoelectrode impedance spectroscopy measures to plant, animal, and human viruses," *IEEE Transactions on Nanobioscience*, vol. 17, no. 2, pp 102–109, Apr 2018, doi: 10.1109/TNB.2018.2826919.

[14] F. Pittino, P. Scarbolo, F. Widdershoven, and L. Selmi, "Derivation and numerical verification of a compact analytical model for the AC admittance response of nanoelectrodes, suitable for the analysis and optimization of impedance biosensors," *IEEE Transactions on Nanotechnology*, vol. 14, no. 4, pp. 709–716, 2015, doi: 10.1109/TNANO.2015.2434106.

[15] H. Haario, M. Laine, A. Mira, and E. Saksman, "DRAM: efficient adaptive MCMC", *Statistics and computing*, vol. 16, no. 4, pp. 339–354, 2006, doi: 10.1007/s11222-006-9438-0.

[16] R. C. Smith, *Uncertainty quantification*, vol. 12 of *Computational Science & Engineering*. Society for Industrial and Applied Mathematics (SIAM), Philadelphia, PA, 2014. Theory, implementation, and applications.